







Biosimilarity and advanced structural characterization of monoclonal antibodies charge variants using capillary zone electrophoresis and mass spectrometry

Lola Alez-Martin^{a,b,*} , Pascal Houzé^{c,d} , Rania Joomun^b , Nathalie Mignet^b ,
Yannis-Nicolas François^a , Rabah Gahoual^b 

^a Laboratoire de Spectrométrie de Masse des Interactions et des Systèmes (LSMIS), Université de Strasbourg, CNRS UMR7140, CMC, Strasbourg, 67081, France

^b Université Paris Cité, CNRS, Inserm, Unité de Technologies Chimiques et Biologiques pour la Santé (UTCBS), 4 Avenue de l'observatoire, Paris, F-75006, France

^c Laboratoire de Toxicologie Biologique, Hôpital Lariboisière, Assistance Publique – Hôpitaux de Paris (AP-HP), Paris, 75010, France

^d Université Paris Cité-INSERM UMRS-1144, Faculté de Sciences Pharmaceutiques et Biologiques, Paris, F-75006, France

ARTICLE INFO

Keywords:

Capillary zone electrophoresis
Monoclonal antibodies
Charge variants
Fraction collection
Post-translational modifications
Mass spectrometry

ABSTRACT

Monoclonal antibodies (mAbs) structural complexity arises from their macromolecular nature and their propensity to undergo post-translational modifications (PTM), potentially leading to the formation of charge variants. Capillary zone electrophoresis (CZE) showed to be particularly relevant for their analysis, however the selectivity provided by CZE separation is not completely elucidated. In this work, CZE-UV analysis was used to characterize charge variants for biosimilars products corresponding to infliximab. Results demonstrated the possibility to identify faint variations between the different products showing its applicability to contribute to mAbs biosimilarity assessment. Enzymatic treatment allowed to attribute the origin of infliximab charge variants. CZE-UV analysis of pembrolizumab showed that none of the five charge variants separated were originating from C-terminal lysine residues and/or N-glycans. To enable further identification, an analytical strategy was developed to achieve CZE-UV fraction collection and enrichment of mAb charge variants followed by systematic offline characterization in CE coupled to tandem mass spectrometry (MS/MS). CE-MS/MS experiments allowed the identification of different types of PTMs such as N-terminal pyroglutamic acid formation and asparagine deamidation for charge variant fractions correlated with decreased mobility. In addition, for the first time succinimide intermediate formation could be successfully characterized using CE-MS/MS data, which could be correlated to increased mobility. Thus, the CZE-UV separation resulted from the synergistic effect of several simultaneous PTMs affecting the apparent mobilities of the charge variants. As a consequence, experiments illustrated the relevance and potential of intact mAbs analysis using CZE-UV to provide an overview of the structural diversity of therapeutic mAbs.

1. Introduction

Monoclonal antibodies (mAbs) have been experiencing a significant expansion within the pharmaceutical industry over the recent years. For instance, a total of 21 therapeutic mAbs received a first approval in 2024 [1]. Therapeutic mAbs are derived from immunoglobulin G (IgG) and are therefore complex macromolecules displaying an extensive diversity of micro-heterogeneities coming from their production process and/or long-time storage. Due to their structural complexity, different types of analytical methods, using a panel of analytical techniques, were

developed to provide a comprehensive characterization over the different aspects defining their structure [2,3]. Especially, mAbs may undergo post-translational modifications (PTM) occurring on amino acids, like methionine (Met) oxidation, asparagine (Asn) deamidation, N-glycosylation or C-terminal lysine (Lys) clipping [4]. PTM may potentially impact the structure, the stability and the functionality of mAbs [5,6]. Thus, they are subject to strict monitoring given their detrimental effect on mAbs stability and potency, as they are considered critical quality attributes (CQA) [7]. For instance, a specific Asn deamidation could be correlated to a disruption of an IgG1 binding to the Fc

* Corresponding author. Laboratoire de Spectrométrie de Masse des Interactions et des Systèmes (LSMIS) Université de Strasbourg, CNRS UMR7140, 4 rue Blaise Pascal, 67081, Strasbourg, France.

E-mail address: lola.alez-martin@etu.unistra.fr (L. Alez-Martin).

<https://doi.org/10.1016/j.talanta.2025.128498>

Received 28 March 2025; Received in revised form 18 June 2025; Accepted 20 June 2025

Available online 20 June 2025

0039-9140/© 2025 Elsevier B.V. All rights reserved, including those for text and data mining, AI training, and similar technologies.

gamma receptor, directly leading to a loss of its antibody-dependent cell-mediated cytotoxicity activity [8]. Moreover, the formation of the Asn⁵⁵ succinimide intermediate and deamidation occurring in the complementarity determining region (CDR) could be successfully linked to a decrease of the binding activity of the mAb to its target [9]. From another perspective, biosimilarity assessment also requires a complete characterization of the mAb biosimilar candidate in order to provide a detailed comparison with the innovator product [10]. The comparison should also demonstrate the absence of significant differences between the two products regarding CQA; otherwise, the absence of impact in terms of bioequivalence should be demonstrated [11].

The inherent structural complexity and variability of mAbs often results in charge variants exhibiting different isoelectric points. Several techniques were implemented for the separation of mAbs charge variants, mainly ion-exchange chromatography [12] and electrophoretic separation techniques such as capillary isoelectric focusing [13]. Also, capillary zone electrophoresis (CZE) demonstrated to be particularly relevant for the separation of mAbs charge variants [14]. CZE-UV performed using a dynamic neutral coating showed the ability to perform robust separation of mAbs charge variants using relatively simple conditions [15]. CZE-UV could be implemented for the analysis of a wide range of mAbs [16], furthermore highlighting the possibility to identify mAbs based on their apparent mobilities and charge variant distribution [17]. Recently, a two-dimensional CE-MS coupling was developed to enable CZE mAbs charge variants separation using non-volatile background electrolyte (BGE), while providing compatibility with ESI-MS analysis [18]. In complement, online digestion using pepsin was implemented which allowed to identify the presence of different types of glycosylation and mass-to-charge ratio (m/z) values compatible with potential occurrence of PTM [19]. As a consequence, despite its relevance, CZE selectivity regarding mAbs charge variants remains to be fully elucidated in order to attribute the structural elements and/or modifications at the origin of their separation.

In the present work, different analytical approaches were implemented in order to study in detail the selectivity of CZE concerning intact mAbs charge variants separation. First, CZE-UV analysis was investigated to perform a rapid biosimilarity assessment of IgG1 infliximab (IFX) innovator and two distinctive biosimilar products, targeting the tumour necrosis factor α . Experiments emphasized the potential of CZE-UV analysis to distinguish mAbs biosimilar products. Various proteolysis treatments were applied to enable the identification regarding charge variants profiles among the different IFX products. Consequently, CZE-UV was performed in the case of IgG4 pembrolizumab (PBZ) which revealed additional structural aspects contributing to the mAbs charge variants separation. To provide a detailed characterization of PBZ charge variants, we designed and implemented a strategy consisting of CZE-UV fraction collection and systematic enrichment. Fractionated charge variants were further characterized using tryptic digestion followed by CE-ESI-MS/MS analysis of the peptide mixtures. Indeed, CE-ESI-MS/MS showed to be particularly adapted to the characterization of mAbs primary structure [2]. Thus, it is demonstrated that from a single analysis, it is possible to achieve complete sequence coverage and a consistent characterization of peptides exhibiting different types of PTM such as N-glycosylation and aspartic acid (Asp) isomerization [20]. PTM occurring on PBZ were precisely identified with CE-ESI-MS/MS including the position of the amino acid modified. Moreover, modification proportions were compared among each charge variants fraction to allow the identification of PTM responsible for intact mAbs mobility changes, providing a novel perspective on CZE-UV charge variants analysis.

2. Materials and methods

2.1. Chemicals

Chemicals used were of high purity grade and purchased from Merck

Sigma-Aldrich (Saint-Louis, MO, USA) if not stated otherwise. Ultra-pure water used to prepare buffers and sample solutions was obtained using an ELGA Purelab UHQ PS water purification system (Bucks, UK). The original products corresponding to the EMA/FDA-approved samples of IFX innovator Remicade® (Merck Sharp and Dohme), the two IFX biosimilars Flixabi® (Biogen) and Remsima® (Celltrion Healthcare), and PBZ (Keytruda®) were purchased or provided by their respective manufacturer. RapiGest SF™ surfactant was purchased from Waters (Milford, MA, USA). Sequencing Grade Modified Trypsin was purchased from Promega (Madison, WI, USA). Carboxypeptidase B was purchased from Roche Diagnostics (Darmstadt, Germany). IgZERO endoglycosidase was purchased from Genovis (Kävlinge, Sweden).

2.2. Sample preparation

Prior to CZE-UV experiments, all mAbs samples were diluted using ultra-pure water to a concentration of 5 mg mL⁻¹. Carboxypeptidase B digestion was realized by diluting 10 µg of mAb sample in a buffer composed of 10 mM NaH₂PO₄, 150 mM NaCl (pH 7.4). Afterward, 1.2 µL of carboxypeptidase B (0.1 mg mL⁻¹) was added to the sample and the mixture was incubated for 2 h at RT. Finally, the treated sample was diluted to a final concentration of 5 mg mL⁻¹ using water. For endoglycosidase treatment, 100 units of IgZERO were added to 50 µg of a mAb in 25 µL of a NaH₃PO₄ buffer (20 mM NaH₃PO₄, 300 mM NaCl, pH 7.4). The sample was incubated for 30 min at 37 °C.

2.3. CZE-UV analysis

CZE-UV experiments were performed using a P/ACE MDQ capillary electrophoresis system (Sciex separations, Darmstadt, Germany). The CE instrument was equipped with a UV detector and operated with 32Karat software (Sciex, Darmstadt, Germany). Separations were performed using a bare-fused silica (BFS) capillary (total length 41 cm, effective length 30,9 cm; 75 µm i.d.) purchased from Polymicro Technologies (Phoenix, AZ, USA). The background electrolyte (BGE) was composed of 556 mM 6- ϵ -aminocaproic acid (EACA), 2.78 mM triethylenetetramine (TETA) and 0.07 % hydroxypropyl methylcellulose (HPMC). A new background electrolyte was prepared each day by adding 462 µL of a 1 % HPMC solution to 6 mL of a 600 mM EACA and 3 mM TETA solution (pH 5.86). New capillaries were conditioned by rinsing at 50 psi with 0.1 M HCl for 10 min, with BGE for 10 min, an electric field of +20 kV was applied for 10 min, and all of those steps were repeated a second time. Then the capillary was flushed for 5 min with BGE at 50 psi. Prior to each injection, the capillary was rinsed with BGE for 5 min at 50 psi. Then the sample was injected for 10 s at 0.5 psi (53.3 nL), and BGE was injected for 6 s at 1 psi. A voltage of +25 kV using normal polarity was applied for the separation during 36 min and the detection was done by UV at 214 nm. The capillary was then rinsed by flushing BGE and then 0.1 M of HCl for 1.5 min at 75 psi each. For overnight storage, the capillary was filled with 10 mM H₃PO₄ (pH 6.9) and the two capillary ends were immersed in ultra-pure water.

2.4. CZE-UV fraction collection and enrichment

For CZE-UV fraction collection, five collection vials previously filled with 100 µL of water in PCR tubes to ensure immersion of the capillary end, were positioned on the CE outlet tray. Initially, sample were separated using conditions described previously (cf. CZE-UV analysis) with a longer BFS capillary (total length 50 cm, effective length 40 cm; 75 µm i.d.). The analysis time t_f (Eq. (1)) was deduced based on the migration times of the separated charge variants. Afterward, fractions were collected in different vials using a low flow hydrodynamic injection of 0.5 psi (319.8 nL/min). A systematic approach was developed to determine the parameters required for precise fraction collection mainly fraction volume and hydrodynamic collection time. Thus, each charge variant peak observed in CZE-UV electropherogram was divided into

two points (peak start/peak end) which delimited the concerned fraction. The apparent mobilities of these points were considered to calculate the position of the corresponding fraction at the end of the electrokinetic separation using Equation (1):

$$x_f = \left(\frac{L_{eff}}{t_m} \right) \times t_f \quad (\text{Eq. 1})$$

where x_f (cm) represented the position of point at the capillary at the end of the separation, L_{eff} (cm) was the effective length of the capillary, t_m (min) represented the migration time corresponding to the point, and t_f (min) corresponded to the final CZE separation time. Consequently, the capillary volume V_F (nL) containing the fraction can be calculated using the position corresponding to the peak start and peak end (Equation (2)):

$$V_F = \left[L_{eff} \times \left(\frac{1}{t_{m1}} - \frac{1}{t_{m2}} \right) \times t_f \right] \times \pi \times (r_{int})^2 \times 10^6 \quad (\text{Eq. 2})$$

where t_{m1} and t_{m2} represented the migration times corresponding to the peak start and peak end respectively (min), and r_{int} (cm) corresponded to the internal radius of the capillary. Finally, the collection time t_{coll} (min) necessary for the fraction using a hydrodynamic injection of 0.5 psi could be deduced (Equation (3)) using the flow rate Q_{coll} (nL/min) obtained from the Hagen-Poiseuille equation:

$$t_{coll} = \frac{V_F}{Q_{coll}} \quad (\text{Eq. 3})$$

The spreadsheet implemented for the determination of fraction collection parameters was made available in [Supporting File 2](#), where one sheet describes the detailed calculation of each parameter, and the second sheet can be directly used. The 0.5 psi pressure was applied for the calculated duration t_{coll} corresponding to the different CZE peaks. For the different samples corresponding to PBZ, the fraction collection was repeated between 40 and 50 times to enrich the fractions. Based on their relative peak areas, the quantity of mAbs charge variants were estimated to be between 0.8 μg for PBZ Basic 1 variant (fraction 1, [Fig. 2](#)) and 8.6 μg in the case of the main charge variant (fraction 3, [Fig. 2](#)) for 50 repetitions.

2.5. Charge variant fractions tryptic digestion for MS analysis

The fractions collected from CZE-UV experiments were first buffer exchanged against 50 mM ammonium bicarbonate (pH 7) by using Amicon® Ultra-0.5 centrifugal filter 30K device (Merck Millipore, Molsheim). Consequently, sample volume was adjusted to 70 μL using 50 mM ammonium bicarbonate. The mAbs charge variants were denatured-reduced-alkylated and digested based on [21]. MABs were denatured with 5 μL of RapiGest SF™ at 0.1 % for 10 min at 80 °C. Then, 10 μL of 50 mM dithiothreitol was added and the sample was left at 80 °C for 20 min for reduction of the disulfide bridges. After the solution was cooled to room temperature, 10 μL of 50 mM iodoacetamide was added and the sample was left in the dark for 20 min for the alkylation of cysteines. Then, 1 μL of trypsin 0.25 g L⁻¹ was added to the sample and left at RT for 3 h. 1 μL of trypsin was added again prior incubation at 37 °C overnight. Finally, the reaction was quenched by adding 1 μL of formic acid 98 %. The peptide mixtures were finally evaporated and reconstituted in 21 μL ammonium acetate 100 mM, pH 4.

2.6. Capillary zone electrophoresis – tandem mass spectrometry analysis

The CZE-ESI-MS/MS analyses were performed on a CESI8000® Capillary Electrophoresis system (Sciex separations, Darmstadt, Germany) coupled with a sheathless CE-ESI-MS interface to a Sciex 5600+ TTOF mass spectrometer (Darmstadt, Germany) operated using Analyst® software (Sciex, Darmstadt, Germany). Separation was performed using a homemade BFS capillary (total length 100 cm; 30 μm i.d.), etched using hydrofluoric acid resulting in a 2 cm porous outlet

positioned inside the cannula of the sheathless interface. The cannula was filled through a second capillary (total length 80 cm; 50 μm i.d.) with BGE consisting of 10 % acetic acid. This allowed the continuity of the electrical field between the CE inlet and outlet electrodes. A pre-concentration step by transient isotachopheresis was included by injecting the peptide digest in a leading electrolyte composed of 100 mM of ammonium acetate (pH 4). 68 nL of sample was injected hydrodynamically (5 psi, 100 s) and the separation was carried out at +23 kV for 60 min. The ESI source parameters were set as follows: ESI voltage -1.5 kV, while gas supplies (GS1 and GS2) were turned off, source heating temperature 100 °C, and curtain gas value 2. Experiments were performed in Top20 information-dependent acquisition (IDA, Sciex), and the accumulation time was 250 ms for MS scans and 80 ms for MS/MS scans, leading to a total duty cycle of 1.9 s. Mass/charge (m/z) range was for 200–2000 in MS and 100–2000 for MS/MS. Data were obtained as .wiff and were analysed through Skyline software. Validation of peptide identification was done manually by annotation of γ - and b -ions from MS/MS spectra. For each category of PTM, the relative proportion of modification was calculated using the MS signals integration corresponding to modified peptides compared to their non-modified counterparts.

3. Results and discussion

3.1. Infliximab biosimilarity assessment using CZE-UV analysis

IFX innovator and two corresponding biosimilars were first characterized independently using CZE-UV analysis. The method implemented a dynamic coating in order to limit the electroosmotic flow (EOF) and prevent protein adsorption on the capillary wall [17]. For IFX innovator (Remicade®), CZE-UV electropherogram showed the separation of three charge variants. As shown in [Fig. 1A](#), the basic 1 variant presented a migration time of 19.8 min, followed by the basic 2 variant at 21.1 min and the main charge variant exhibited a migration time of 22.7 min. Finally, the electropherogram showed a couple of minor acid variants with migration times ranging from 23.3 to 25.0 min. Regarding the first IFX biosimilar (Remsima®), CZE-UV data exhibited similar peaks corresponding to IFX main and basic variants. However, the distribution of charge variants differed between IFX innovator and IFX biosimilars ([Fig. S1](#)). In addition, acidic variants and additional variants between 25 and 27 min were found in higher proportion in the biosimilars ([Fig. 1A](#)). In the case of the second IFX biosimilar (Flixabi®), the early basic variant presenting a migration time of 19.8 min could not be detected and the second basic variant showed an extremely low signal. Thus, the detection of the main variants was convincing using CZE-UV, as the results provided equivalent migration times for the main variant and detectable signal for the acidic variants. The repeatability of CZE-UV analysis appeared to be relevant for the analysis of IFX charge variants, enabling comparative study. Results highlighted the ability of the electrokinetic method to distinguish faint differences between samples composed of the same type of mAbs.

Various experiments were performed in order to attribute the modification responsible for the charge variants differences observed for the products corresponding to IFX. The different mAbs samples were submitted to enzymatic proteolysis using carboxypeptidase B which hydrolyses basic amino acid residues such as C-terminal arginine (Arg) or Lysine (Lys) [22]. Consequently, IFX samples were analysed using the CZE-UV method. Concerning Remicade® and Remsima®, the enzymatic treatment resulted in the absence of IFX basic variants as shown in [Fig. 1B](#). Therefore, nearly the entire sample content was composed of the main charge variant of IFX. The amino acid sequence corresponding to the heavy chain of IFX contains a C-terminal Lys residue. As a consequence, the comparison of CZE-UV obtained from initial samples and digested samples allowed to attribute the origin of basic charge variants to C-terminal Lys clipping. Indeed, Lys are basic residues exhibiting a positive charge at the BGE pH (5.86) for the CZE-UV analysis conditions.

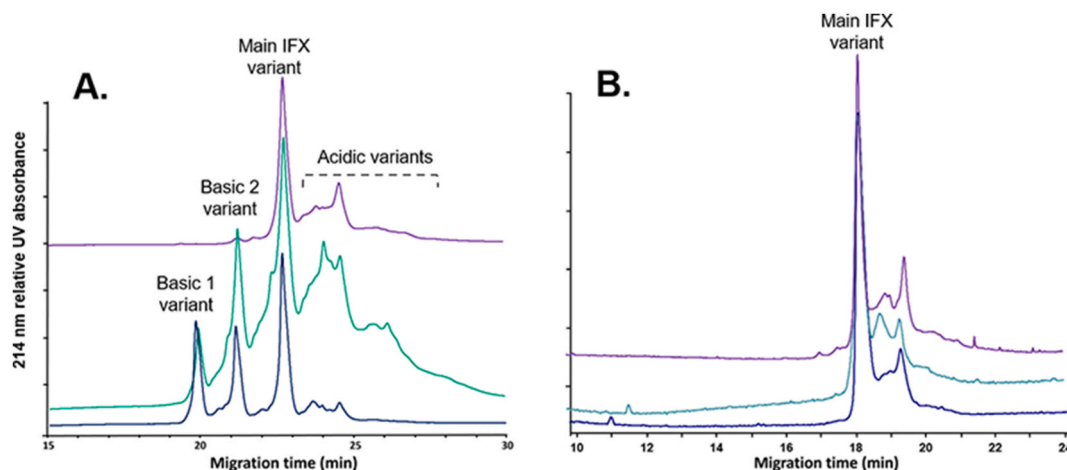


Fig. 1. Electropherograms obtained from the CZE-UV analysis of (A) intact formulation of IFX innovator (Remicade®, dark blue trace) and two approved IFX biosimilars Flixabi® (purple trace) and Remsima® (green trace) (separation voltage +20 kV) and (B) the corresponding IFX products after carboxypeptidase B digestion (separation voltage +25 kV). (For interpretation of the references to colour in this figure legend, the reader is referred to the Web version of this article.)

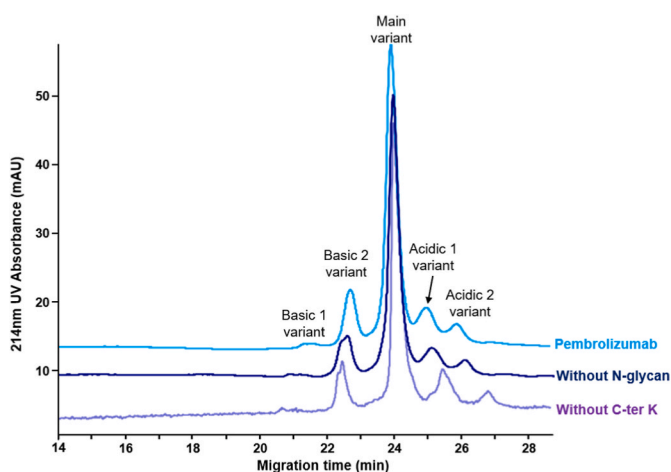


Fig. 2. Electropherograms obtained from CZE-UV analysis of intact formulation of PBZ (light blue trace), PBZ sample undergoing PNGase F digestion (dark blue trace) and PBZ sample treated using carboxypeptidase B proteolysis (purple trace) (capillary total length: 41 cm). (For interpretation of the references to colour in this figure legend, the reader is referred to the Web version of this article.)

Due to the polarity of the CZE separation, the presence of C-terminal Lys increased the mobility of basic variants resulting in shorter migration times (Fig. 1A). Because mAbs are composed of two identical heavy chains, the first peak (basic 1) could be attributed to the presence of C-terminal Lys on both chains, while the second peak (basic 2) corresponded to the loss of a single Lys residue. Finally, the main peak could be attributed to IFX bearing no C-terminal Lys on its two heavy chains. Note that C-terminal Lys clipping on mAbs could be identified similarly at the Fc/2 scale [23]. In the case of IFX biosimilar Flixabi®, as previously mentioned, the CZE-UV analysis did not show significant peaks for IFX charge variants corresponding to basic species (Fig. 1A). Consequently, CZE-UV analysis of Flixabi® sample undergoing carboxypeptidase B proteolysis could not involve major changes of the electropherogram (Fig. 1B). Therefore, the comparison of CZE-UV results in the case of Flixabi® revealed the absence of charge variants presenting C-terminal Lys. Finally, it is important to note that the different IFX samples submitted to proteolysis demonstrated afterward highly similar charge variants profiles obtained from CZE-UV electropherograms as illustrated in Fig. 1B.

From the perspective of IFX biosimilarity assessment, experiments demonstrated that differences characterized by CZE-UV data between IFX innovator Remicade® and the two corresponding biosimilar Remsima® and Flixabi® were originating from dissimilarities regarding C-terminal Lys variants distribution. This modification represents a phenomenon naturally occurring on IgG to a larger extent. As such, it was reported to occur in a similar manner for therapeutic mAbs, in particular it appeared to be impacted by the production process [24]. Nevertheless, this modification could not be correlated to a significant impact of the binding affinity of mAbs to their corresponding antigen or the occurrence of adverse effects. As a consequence, the different IFX products characterized could be considered from this aspect as bio-equivalent, explaining their categorization as biosimilar [25].

CZE-UV conditions used for mAbs charge variants analysis demonstrated the possibility to unambiguously identify the nature of IFX products, either innovator or biosimilars, based on their charge variants relative distribution. That characteristic is particularly interesting due to the absence of sample treatment and relatively short analysis time. Therefore, CZE-UV analysis could be a relevant alternative in early experiments performed in the context of mAbs biosimilarity assessment due to the straightforward characteristics and transposability of the method. Finally, results allowed to prove the origin of major IFX variants using limited proteolysis to complement the identification of charge variants.

3.2. Pembrolizumab charge variant analysis using CZE-UV

PBZ formulation was analysed using the CZE-UV method similarly to IFX. As illustrated in Fig. 2, the electropherogram corresponding showed the detection of PBZ main charge variants having a migration time of 23.9 min. Two basic variants exhibiting faster mobilities could also be detected at 21.5 and 22.7 min respectively, and two acidic variants were identified for migration times 25.0 and 25.9 min (Fig. 2). Note that, CZE-UV analysis showed significant differences in terms of detection windows for PBZ charge variants and distribution compared to IFX products (Fig. 1A). That characteristic was explained due to the difference of isoelectric point and inherent charge variants composition between PBZ and IFX. Thus, CZE-UV experiments allowed to highlight the possibility using this technique to identify different types of mAbs based on the conjunction of their charge variants migrations times and relative proportions. To further confirm this characteristic of CZE-UV analysis, a sample of interleukin-2 (IL-2) was analysed as a negative control using similar conditions. Analysis of IL-2 exhibited a totally different electropherogram compared to mAbs, especially presenting a single charge

variant (Fig. S2).

In order to further identify the origin of the different PBZ charge variants, the sample was submitted to carboxypeptidase B proteolysis followed by CZE-UV analysis. As emphasized in Fig. 2, the proteolytic treatment did not affect the CZE-UV electropherograms. Therefore, in the case of PBZ, charge variants could not be attributed to C-terminal Lys variants unlike IFX. Similarly, PBZ formulation sample was undergoing PNGase F endoglycosidase digestion to systematically remove N-glycans typically present on mAbs heavy chains [26]. In this case as well, PNGase F treatment did not involve any changes of CZE-UV electropherograms which allowed to exclude the origin of the charge variants as coming from different glycoforms (Fig. 2).

As a consequence, CZE-UV experiments clearly suggested that charge variants composing PBZ formulation were due to variabilities which differed from C-terminal Lys clipping or the expression of various N-glycans. Still, the selectivity provided by the CZE method proved to ensure the efficient separation of PBZ charge variants. Unfortunately, the methodology using limited digestion adopted in the case of IFX was not conclusive here. Therefore, further investigations were required in order to fully attribute the selectivity of the electrokinetic separation regarding mAbs charge variants and to identify PBZ species.

3.3. Implementation of CZE-UV fractions collection and enrichment

Likewise all types of proteins, mAbs may be affected by amino acid post-translational modifications (PTM) which could potentially result in isoelectric point shifting. In order to investigate this hypothesis in the context of PBZ and identify the PTM at the origin of the charge variant separation, a strategy enabling fraction collection from the CZE-UV separation was developed. The charge variants of PBZ fractionated during CZE separation, were collected and submitted to trypsin proteolysis. The peptide mixtures obtained were analysed using subsequent offline CE-MS/MS in order to provide a bottom-up characterization of PTM and correlate differences among separated fractions.

The analytical workflow developed to achieve mAbs charge variants CZE fractionation and enrichment is represented in Fig. 3. Concerning CZE-UV fractionation and fraction collection, the method was performed in two steps. First, the electrokinetic separation was applied similarly to previous CZE-UV in order to enable the migration and simultaneous separation to the detector of the charge variant. On the CE instrumentation, the UV detection window is swerved ahead from the effective outlet of the capillary. Therefore, the CZE separation time was adjusted to allow the separated fractions to remain between the UV detector and the capillary outlet. Consequently, the second step

consisted of the collection of the separated fractions in different vials using the hydrodynamic injection system which equipped the CE instrument as illustrated in Fig. 3. To provide an accurate collection of the different fractions, a systematic approach was designed to tune the parameters of the method involved in the collection mainly the injection pressure and duration. Fundamentally, the dimensions of the CZE capillary and the migration times corresponding to the different peaks were taken into account in order to determine the position of each fraction inside the capillary at the end of the analysis. Afterward, it could be possible to deduce using fluidic equations the volume corresponding to each fraction depending on their respective peak width, and the injection timing required to collect the corresponding fraction. The fraction collection approach is detailed in the materials and methods section, and a useable spreadsheet was made available as supporting information. This approach was particularly relevant because it could be applied without any additional or specific instrumentation. In addition, it provided the versatility necessary to address minor variabilities for instance in case of capillary change.

Using the developed method, PBZ charge variants were separated into five fractions collected independently (Fig. S3). One of the main limitations of CE is the restricted quantity injected even in the case of concentrated samples. As a consequence, CZE-UV fractionation of PBZ was repeated several dozens of times in order to enrich fractions to amounts compatible with the subsequent CE-MS/MS characterization. Electropherograms showed the excellent repeatability of the separation with migration times standard deviation mean of 0.18 min for 12 subsequent analyses (Fig. S3). Such level of robustness was explained by the efficiency of the dynamic coating which prevents protein adsorption and modulated EOF. Also, the composition of the BGE revealed to be particularly stable while presenting a limited conductivity. Conveniently, CZE separation repeatability was the sine *qua non* condition to achieve fraction enrichment. To validate the fraction collection approach, a 40 repetitions fraction enrichment was performed for a sample of PBZ. Consequently, each fraction was analysed independently using the CZE-UV method. As presented in Fig. 4, the electropherograms obtained for the different fractions demonstrated the successful isolation of the different charge variants corresponding to PBZ. Especially, the CZE-UV analysis of the first two fractions composed of basic variant fractions (Basic 1, Basic 2) showed only a single peak. For the analysis of the third fraction, a large majority of the signal was found to correspond to PBZ main charge variant as expected (Fig. 4). Finally, the CZE-UV analysis of the last two fractions enabled the identification of peaks attributed initially to acidic variants (Acidic 1, Acidic 2). Some minor contamination could be observed in particular for fractions containing

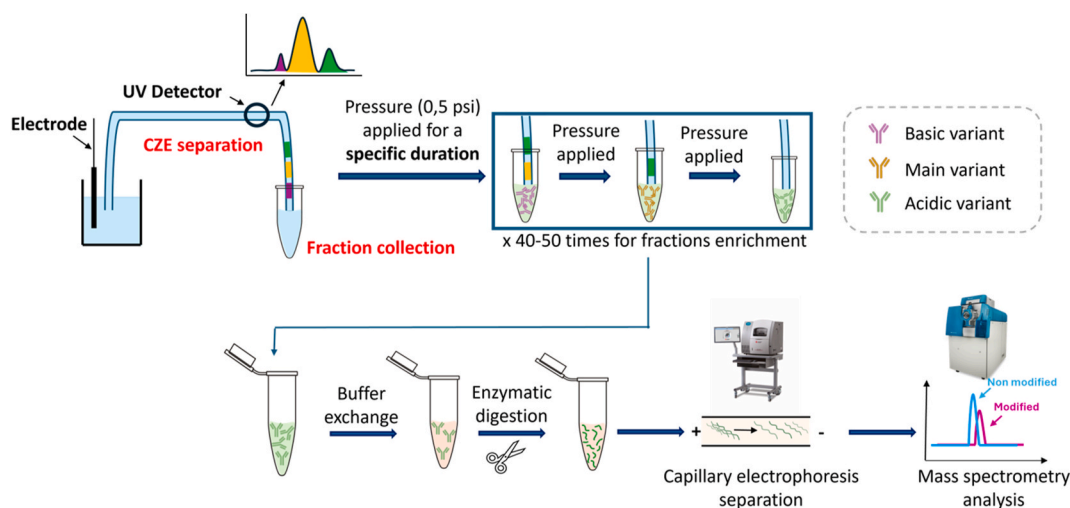


Fig. 3. Schematic representation of the analytical workflow developed for the structural characterization of PBZ charge variants using CZE-UV fraction collection followed by offline CZE-ESI-MS/MS analysis.

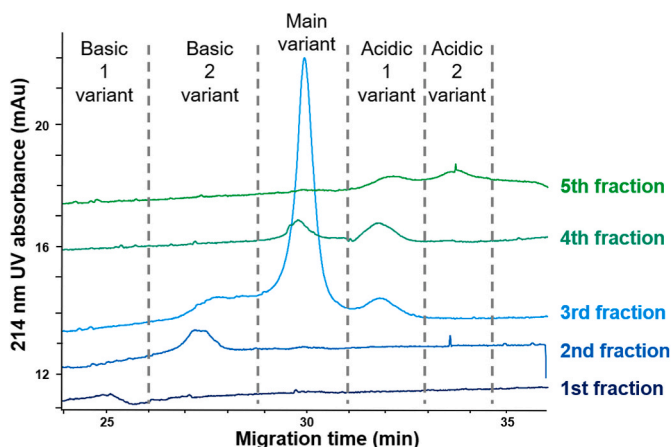


Fig. 4. CZE-UV electropherograms obtained from the analysis of samples corresponding to the five different fractions collected for PBZ sample. Each fraction was obtained from a 40-time enrichment using the CZE-UV analytical workflow developed (cf. Materials and methods section).

acidic variants. This phenomenon was attributed to the initial CZE separation which could not enable a baseline separation of PBZ acidic variants as shown in Fig. 2. Also, some faint longitudinal diffusion could be involved due to the hydrodynamic fraction collection, however it should be nearly negligible because of the narrow capillary internal diameter. The last fraction corresponding to the acidic 2 variant was significantly impacted from contamination of the previous fraction due to diffusion (Fig. 4). Thus, further MS/MS characterization of the last fraction was not considered as it would not be representative of the acidic 2 charge variant.

3.4. CESI-MS/MS analysis of the fractionated charge variants

CZE-UV fractions collected were first submitted to centrifugal filtration to remove EACA, originating from the BGE, to prevent trypsin inhibition [27]. Charge variants composing the different fractions were then digested into peptides followed by CE-MS/MS analysis. CE-MS/MS data were used to characterize the occurrence of PTM specifically for pembrolizumab charge variants separated using the CZE-UV method [28]. Peptides considered for the characterization of PTM are summarized in Table 1. Note that peptides were identified based on their m/z ratio and fragment annotations from MS/MS data. For the different fractions, results allowed to achieve an extensive characterization of pembrolizumab charge variants primary structure. Indeed, data allowed to obtain sequence coverage up to 100 % for the light chain and 75.20 % for the heavy chain. Therefore, peptides potentially exhibiting PTM of interest could be identified in a robust manner even in the case of the fraction representing lowly abundant variants (Fig. 4).

Table 1

List of pembrolizumab tryptic peptides potentially exhibiting PTM characterized using CE-MS/MS analysis. Identification was considered positive based on m/z measurement (mass accuracy <10 ppm) and fragment interpretation using MS/MS spectra.

Peptide	Modification position	Theoretical m/z	PTM	Theoretical m/z after modification
QVQLVQSGVEVK	Gln ¹ (HC)	657.3748	Pyroglutamate	648.8598
QAPGQGLEWGGINPNSGGTTFNEK	Asn ⁵⁵ (HC)	1302.1008	Deamidation	1302.5908
SLQFDDTAVYYCAR	Asp ⁹⁰ (HC)	854.8747	Succinimide	845.8672
VVSVLTVLHQDWLNGK	Asn ³¹⁵ (HC)	904.5069	Deamidation	904.9969
VSNK	Asn ³²⁵ (HC)	447.2562	Deamidation	448.2362
GFYPSDIAVEWESNGQPENNYK	Asn ³⁸⁴ (HC)	1272.5693	Deamidation	1273.0593
GFYPSDIAVEWESNGQPENNYK	Asn ³⁸⁴ ;Asn ³⁸⁸ (HC)	1272.5693	Deamidations	1273.5493
TTPPVLDSDGSFFLYSR	Asp ⁴⁰¹ (HC)	951.4676	Succinimide	942.4601
SLSLSLG(K)	Lys ⁴⁴⁷ (HC)	804.4825	Truncation	676.3876
SGTASVVCLLNNFYPR	Asn ¹⁴¹ (LC)	899.4405	Deamidation	899.9305
VDNALQSGNSQESVTEQDSK	Asp ¹⁷¹ (LC)	1068.4880	Succinimide	1059.4805

CE-MS/MS data were used to identify the heavy chain N-glycosylation expressed by the different charge variants. Thus, MS/MS allowed the unambiguous identification of the 4 major N-glycans G0F, G1F, G2F and G0 in all the fractions. Based on the extracted ion electropherograms corresponding to the various glycopeptides, the relative proportion of glycan G0F was found to be 78 %, meanwhile the proportion of G1F represented 16 %, G2F 1 % and G0 5 % (Fig. S4). Interestingly, N-glycosylations identified were similar for the different fractions in terms of glycans nature and relative distribution. As a consequence, N-glycans incorporated into the mAbs heavy chain were not involved in the separation of charge variants observed on CZE-UV electropherograms. Moreover, this interpretation was in agreement with the absence of changes in CZE-UV charge variants separation consequently to N-glycan removal using endoglycosidase (Fig. 2). It is important to note also that N-glycosylation distribution obtained from CE-MS/MS was consistent with previous reports [29]. Therefore, it indicated that CZE-UV fraction collection and enrichment reflected a consistent glycodistribution without the introduction of experimental biases.

Similarly, the C-terminal peptide of the heavy chain was identified using CE-MS/MS. For the samples corresponding to the different charge variants, only the C-terminal peptide free from Lys residue (SLSLSLG) could be identified. It could be concluded that PBZ did not present C-terminal Lys which could be involved in charge variants diversity. This observation was in line with the absence of changes in CZE-UV charge variants after the digestion of PBZ with the carboxypeptidase B.

The cyclization of glutamine in N-terminal position (Gln¹) into pyroglutamic acid was identified for PBZ heavy chain using CE-MS/MS data. As expected, MS/MS information showed a mass shift of -17.03 Da supported by the complete annotation of the amino acid sequence using fragmentation spectra (Table 1). As emphasized in Fig. 5A, fractions F1 and F2 presented minimal and relatively close levels of pyroglutamic acid formation. For fractions F3 and F4, corresponding to lower mobilities charge variants, higher levels of pyroglutamic acid could be measured from CE-MS/MS. Therefore, results from the comparison of Gln¹ cyclization levels for the different fractions pointed that the modification tend to lower the mobility of the corresponding charge variant. Indeed, the modification involves the formation of pyroglutamic acid which should prevent protonation of the N-terminal amine group and generate the loss of a positive charge compared to the unmodified PBZ variant [30]. Thus, this modification induces a decrease of its apparent mobility in CZE-UV. Note that for CE-MS/MS experiments performed on digested peptides, N-terminal pyroglutamic acid formation enabled the separation of the unmodified peptide from its modified counterpart also due to lower mobility [31].

CE-MS/MS analysis enabled also to achieve the characterization of Asn deamidation leading to the formation of Asp. The identification of modified Asn residues was achieved from the m/z ratio, presenting a mass difference of $+0.98$ Da between the modified and the unmodified peptide. In total, six Asn residues exhibited deamidation based on CE-MS/MS analysis of the fractions collected for PBZ (Table 1). Results

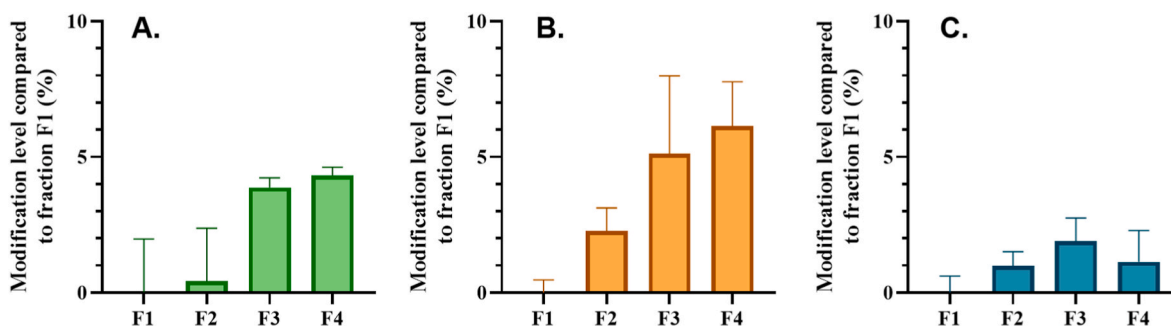


Fig. 5. Evolution of modification levels estimated using CE-MS/MS analysis for the different fractions corresponding to PBZ charge variants fractionated for (A) Pyroglutamic acid formation of N-terminal glutamine, (B) Deamidation for six Asn residues and (C) Succinimide formation from three Asp residues. Modification levels are represented in comparison to fraction F1. CZE-UV fraction collection was performed in triplicates ($n = 40$ enrichments each), and fraction samples were systematically analysed using CE-MS/MS in triplicates.

presented in Fig. 5B demonstrate an increase of deamidation level for the different fractions. Therefore, the occurrence of Asn deamidation could be correlated with a decrease of mobility among the PBZ charge variants, which translated into longer migration times in CZE-UV analysis (Fig. 2). This change regarding the mobility of PBZ charge variants could be explained by the modification of neutral Asn into Asp residues exhibiting a negative charge (pK_a 3.86) due to the BGE conditions (pH 5.86). Because of the polarity applied for the CZE-UV separation, additional negative charges led to longer migration times for the corresponding charge variants. In addition, CE-MS/MS analysis showed that peptides experiencing Asn deamidation had longer migration time, about 0.3 min, compared to the equivalent without modification enabling systematic baseline separation. However, it is important to note that several Asn residues demonstrated significant modification, therefore the PBZ charge variants separation observed from CZE-UV separation could not be attributed to the modification of a specific amino acid.

Similarly to previous PTM, experiments could be used to obtain the characterization of Asp residue modification into succinimide (Asu). Thus, CE-MS/MS data demonstrated that the formation of Asu entailed a mass difference of -18.01 Da between the modified peptide and its intact equivalent. Also, the occurrence of the modification led to a shorter migration time in CE-MS/MS electropherograms which contributed to their unambiguous identification (Fig. 6A). CE-MS/MS results allowed the identification of Asu intermediate formation for Asp¹⁷¹, Asp⁹⁰ and Asp⁴⁰¹ (Table 1). In each case, MS/MS spectra allowed to prove the presence of the modification and precisely determine its localization as presented for Asp⁹⁰ in Fig. 6B. It is the first time that a succinimide intermediate characterization could be achieved using CE-MS/MS analysis therefore enriching even further the PTM that can be identified using this method. The proportion of Asu was found to be

increasing for the first three fractions, with the highest modification level recorded in the case of fraction F3 corresponding to PBZ main variant (Fig. 5C). Interestingly, fraction F4 demonstrated lower levels of Asp modification compared to fraction F3. Due to the BGE used for CZE-UV analysis, Asp residue should exhibit a negative charge, whereas Asu intermediate involves a modification into a neutral specie, therefore increasing the mobility of the charge variant. Thus, the impact of Asu formation from Asp on mAbs charge variant mobility is in opposition to the one involved from Asn deamidation. This observation explained the higher proportions of Asu intermediate formation in fraction F3 compared to fraction F4. Indeed, charge variants presenting at the same time significant Asn deamidation and Asu intermediate formation migrated in fraction F3 because of the counter-balancing effects of the two modifications.

The characterization of the primary structure of intact PBZ charge variants, fractionated using CZE-UV, could be successfully performed using CE-MS/MS analysis. The data allowed to characterize PTM level variations among the different PBZ fractions collected and correlated their impact of the CZE-UV separation. Thus, results allowed to attribute the occurrence of N-terminal pyroglutamic acid formation with a decrease of the charge variant mobility and longer migration time. From another aspect, Asn deamidation decreased the mobility of the affected charge variants. On the contrary, the formation of Asu intermediate from Asp residue led to a mobility increase in CZE-UV. The study revealed that in the case of PBZ, separation of the charge variants did not originate from the modification of a specific residue, but on the conjunction of different types of PTM occurring potentially at the same time on different amino acids. The direct consequence was that each CZE-UV fraction collected contained a combination of species presenting relatively close charge in solution. In addition, each type of PTM occurring on PBZ primary structure impacted differently the mobility of

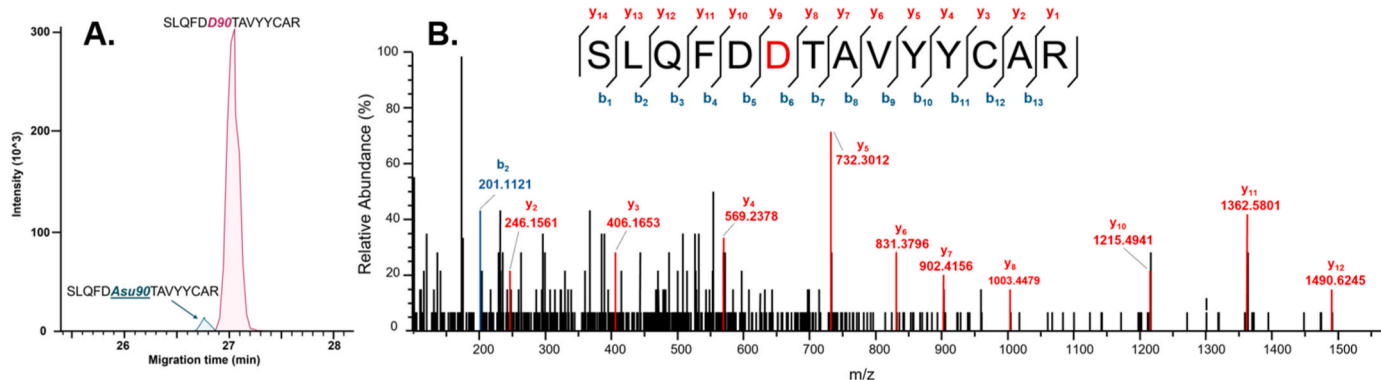


Fig. 6. (A) CE-MS/MS extracted ion electropherograms of the peptide exhibiting Asu formation for Asp⁹⁰ (26.77 min) and the non-modified peptide (27.04 min) obtained from the analysis of a fraction collected of PBZ. (B) MS/MS Spectra of SLQFDDTAVYYCAR with succinimide formation on Asp⁹⁰.

the charge variant. As a consequence, they demonstrated a synergetic effect on the mobility observed on CZE-UV electropherograms. This conclusion clearly highlighted that CZE-UV remains an excellent method for the separation of mAbs charge variants, and demonstrated the complementarity with peptide centric characterization realized using CE-MS/MS.

4. Conclusion

An integrated analytical strategy could be developed for the separation and structural characterization of charge variants. The implementation of CZE-UV proved to be particularly relevant for the analysis of intact mAbs charge variants. Thereby, experiments enabled to take advantage of the CZE-UV separation selectivity to provide rapid and confident identification of the nature of mAbs samples. Application to IFX demonstrated for the first time the possibility, using CZE-UV analysis, to distinguish unambiguously different biosimilar products corresponding to the same mAb. Therefore, it highlighted the potential of electrokinetic separation in the early stages of mAbs biosimilarity assessment. Different approaches could be explored in order to identify structural variabilities responsible for mAbs charge variants separation. Limited digestion allowed to attribute the influence of C-terminal Lys variants on the CZE separation, further justifying the bioequivalence between IFX products. To attribute the complex charge variants of PBZ, a systematic tailor-made CZE-UV fraction collection was developed in order to realize subsequent PTM identification using CE-MS/MS analysis. Results provided the advanced primary structure characterization of fractionated mAbs giving access to PTM localization and modification levels. Especially, the characterization of Asp modification to the Asu intermediate using CE-MS/MS analysis could be reported for the first time. Experiments allowed to attribute variations concerning PTM levels for the different charge variants to their respective impact on the initial CZE separation. The study demonstrated that PTM like N-terminal pyroglutamic acid formation or Asn deamidation involved a decrease of mAbs mobilities, whereas Asu intermediate formation led to the opposite effect. Therefore, PBZ charge variants resulted from the conjunction of different types of PTM producing a synergetic effect on the charge variant mobilities. Thus, mAbs exhibited a significant number of PTM potentially generating charge variants. In addition, PTM diversity and modification levels appeared mAb dependent which justified the necessity to perform mAbs charge variants analysis in the context of their structural characterization. Consequently, intact mAbs analysis using CZE-UV represents a relevant alternative to provide a general overview of the inherent diversity of mAbs variants.

CRedit authorship contribution statement

Lola Alez-Martin: Writing – review & editing, Writing – original draft, Methodology, Investigation, Formal analysis. **Pascal Houzé:** Writing – review & editing, Supervision. **Rania Joomun:** Investigation. **Nathalie Mignet:** Writing – review & editing, Supervision. **Yannis-Nicolas François:** Writing – review & editing, Methodology, Conceptualization. **Rabah Gahoual:** Writing – review & editing, Writing – original draft, Methodology, Investigation, Conceptualization.

Declaration of competing interest

The authors declare that they have no competing financial interests or personal relationships that could have appeared to influence the work reported in this paper.

Acknowledgements

The authors would like to thank the Chemical Sciences Doctoral School of the University of Strasbourg (ED222) for funding the PhD project of Lola Alez-Martin.

Appendix A. Supplementary data

Supplementary data to this article can be found online at <https://doi.org/10.1016/j.talanta.2025.128498>.

Data availability

The data that has been used is confidential.

References

- [1] S. Crescioli, H. Kaplon, L. Wang, J. Visweswaraiha, V. Kapoor, J.M. Reichert, Antibodies to watch in 2025, *mAbs* 17 (1) (2025 Dec 31) 2443538, <https://doi.org/10.1080/19420862.2024.2443538>.
- [2] A.M. Belov, L. Zang, R. Sebastiano, M.R. Santos, D.R. Bush, B.L. Karger, et al., Complementary middle-down and intact monoclonal antibody proteoform characterization by capillary zone electrophoresis – mass spectrometry, *Electrophoresis* 39 (16) (2018 Aug) 2069–2082, <https://doi.org/10.1002/elps.201800067>.
- [3] A. Beck, V. D'Atri, A. Ehkirch, S. Fekete, O. Hernandez-Alba, R. Gahoual, et al., Cutting-edge multi-level analytical and structural characterization of antibody-drug conjugates: present and future, *Expert Rev. Proteomics* 16 (4) (2019 Apr 3) 337–362, <https://doi.org/10.1080/14789450.2019.1578215>.
- [4] W. Li, J.L. Kerwin, J. Schiel, T. Formolo, D. Davis, A. Mahan, et al., Structural elucidation of post-translational modifications in monoclonal antibodies, in: J. E. Schiel, D.L. Davis, O.V. Borisov (Eds.), *ACS Symposium Series*, American Chemical Society, Washington, DC, 2015, pp. 119–183.
- [5] Y. Yan, H. Wei, Y. Fu, S. Jusuf, M. Zeng, R. Ludwig, et al., Isomerization and oxidation in the complementarity-determining regions of a monoclonal antibody: a study of the modification–structure–function correlations by hydrogen–deuterium exchange mass spectrometry, *Anal. Chem.* 88 (4) (2016 Feb 16) 2041–2050, <https://doi.org/10.1021/acs.analchem.5b02800>.
- [6] B. Wei, K. Berning, C. Quan, Y.T. Zhang, Glycation of antibodies: modification, methods and potential effects on biological functions, *mAbs* 9 (4) (2017 May 19) 586–594, <https://doi.org/10.1080/19420862.2017.1300214>.
- [7] P. Legrand, S. Dufaj, N. Mignet, P. Houzé, R. Gahoual, Modeling study of long-term stability of the monoclonal antibody infliximab and biosimilars using liquid-chromatography–tandem mass spectrometry and size-exclusion chromatography–multi-angle light scattering, *Anal. Bioanal. Chem.* 415 (1) (2023 Jan) 179–192, <https://doi.org/10.1007/s00216-022-04396-7>.
- [8] X. Lu, L.A. Machiesky, N. De Mel, Q. Du, W. Xu, M. Washabaugh, et al., Characterization of IgG1 Fc deamidation at asparagine 325 and its impact on antibody-dependent cell-mediated cytotoxicity and FcγRIIIa binding, *Sci. Rep.* 10 (1) (2020 Jan 15) 383, <https://doi.org/10.1038/s41598-019-57184-2>.
- [9] B. Yan, S. Steen, D. Hambly, J. Valliere-Douglass, T.V. Bos, S. Smallwood, et al., Succinimide formation at Asn 55 in the complementarity determining region of a recombinant monoclonal antibody IgG1 heavy chain, *J Pharm Sci* 98 (10) (2009 Oct) 3509–3521, <https://doi.org/10.1002/jps.21655>.
- [10] T. Reinert, P. Houzé, N. Mignet, Y.N. Francois, R. Gahoual, Post-translational modifications comparative identification and kinetic study of infliximab innovator and biosimilars in serum using capillary electrophoresis-tandem mass spectrometry, *J. Pharm. Biomed. Anal.* 234 (2023 Sep) 115541, <https://doi.org/10.1016/j.jpba.2023.115541>.
- [11] European Medicines Agency, Guideline on similar biological medicinal products. https://www.ema.europa.eu/en/documents/scientific-guideline/guideline-similar-biological-medicinal-products-rev1_en.pdf, 2025. (Accessed 28 March 2025).
- [12] S.Y. Jing, J.X. Gou, D. Gao, H.B. Wang, S.J. Yao, D.Q. Lin, Separation of monoclonal antibody charge variants using cation exchange chromatography: resins and separation conditions optimization, *Sep. Purif. Technol.* 235 (2020 Mar) 116136, <https://doi.org/10.1016/j.seppur.2019.116136>.
- [13] A. Goyon, M. Excoffier, M.C. Janin-Bussat, B. Bobaly, S. Fekete, D. Guilleme, et al., Determination of isoelectric points and relative charge variants of 23 therapeutic monoclonal antibodies, *J. Chromatogr. B* 1065–1066 (2017 Oct) 119–128, <https://doi.org/10.1016/j.jchromb.2017.09.033>.
- [14] A. Goyon, Y.N. Francois, O. Colas, A. Beck, J.L. Veuthey, D. Guilleme, High-resolution separation of monoclonal antibodies mixtures and their charge variants by an alternative and generic CZE method, *Electrophoresis* 39 (16) (2018 Aug) 2083–2090, <https://doi.org/10.1002/elps.201800131>.
- [15] Y. He, C. Isele, W. Hou, M. Ruesch, Rapid analysis of charge variants of monoclonal antibodies with capillary zone electrophoresis in dynamically coated fused-silica capillary: electrodriven separations, *J Sep Sci* 34 (5) (2011 Mar) 548–555, <https://doi.org/10.1002/jssc.201000719>.
- [16] R. Wiesner, H. Zagst, W. Lan, S. Bigelow, P. Holper, G. Hübner, et al., An interlaboratory capillary zone electrophoresis-UV study of various monoclonal antibodies, instruments, and ϵ -aminocaproic acid lots, *Electrophoresis* 44 (15–16) (2023 Aug) 1247–1257, <https://doi.org/10.1002/elps.202200284>.
- [17] P. Legrand, O. Dembele, H. Alamil, C. Lamoureux, N. Mignet, P. Houzé, et al., Structural identification and absolute quantification of monoclonal antibodies in suspected counterfeiters using capillary electrophoresis and liquid chromatography-tandem mass spectrometry, *Anal. Bioanal. Chem.* 414 (8) (2022 Mar) 2699–2712, <https://doi.org/10.1007/s00216-022-03913-y>.
- [18] K. Jooß, J. Hühner, S. Kiessig, B. Moritz, C. Neustüß, Two-dimensional capillary zone electrophoresis–mass spectrometry for the characterization of intact

- monoclonal antibody charge variants, including deamidation products, *Anal. Bioanal. Chem.* 409 (26) (2017 Oct) 6057–6067, <https://doi.org/10.1007/s00216-017-0542-0>.
- [19] J. Schlecht, K. Jooß, B. Moritz, S. Kiessig, C. Neusüß, Two-dimensional capillary zone electrophoresis-mass spectrometry: intact mAb charge variant separation followed by peptide level analysis using In-Capillary digestion, *Anal. Chem.* 95 (8) (2023 Feb 28) 4059–4066, <https://doi.org/10.1021/acs.analchem.2c04578>.
- [20] R. Gahoual, A. Beck, Y.N. François, E. Leize-Wagner, Independent highly sensitive characterization of asparagine deamidation and aspartic acid isomerization by sheathless CZE-ESI-MS/MS: characterization of Asn and Asp PTMs by CZE-ESI-MS, *J. Mass Spectrom.* 51 (2) (2016 Feb) 150–158, <https://doi.org/10.1002/jms.3735>.
- [21] T. Reinert, R. Gahoual, N. Mignet, A. Kulus, M. Allez, P. Houzé, et al., Simultaneous quantification and structural characterization of monoclonal antibodies after administration using capillary zone electrophoresis-tandem mass spectrometry, *J. Pharm. Biomed. Anal.* 233 (2023 Sep) 115446, <https://doi.org/10.1016/j.jpba.2023.115446>.
- [22] R.P. Ambler, [14] *Enzymic hydrolysis with carboxypeptidases*, in: *Methods in Enzymology*, Elsevier, 1967, pp. 155–166.
- [23] Y.N. François, M. Biacchi, N. Said, C. Renard, A. Beck, R. Gahoual, et al., Characterization of cetuximab Fc/2 dimers by off-line CZE-MS, *Anal. Chim. Acta* 908 (2016 Feb) 168–176, <https://doi.org/10.1016/j.aca.2015.12.033>.
- [24] L.W. Dick, D. Qiu, D. Mahon, M. Adamo, K. Cheng, C-terminal lysine variants in fully human monoclonal antibodies: investigation of test methods and possible causes, *Biotechnol. Bioeng.* 100 (6) (2008 Aug 15) 1132–1143, <https://doi.org/10.1002/bit.21855>.
- [25] V. Faid, Y. Leblanc, M. Berger, A. Seifert, N. Bihoreau, G. Chevreux, C-terminal lysine clipping of IgG1: impact on binding to human FcγRIIIa and neonatal Fc receptors, *Eur J Pharm Sci* 159 (2021 Apr) 105730, <https://doi.org/10.1016/j.ejps.2021.105730>.
- [26] F.S. Van De Bovenkamp, N.I.L. Derksen, P. Ooijevaar-de Heer, T. Rispens, The enzymatic removal of immunoglobulin variable domain glycans by different glycosidases, *J. Immunol.* 467 (2019 Apr) 58–62, <https://doi.org/10.1016/j.jim.2019.02.005>.
- [27] L. Kupcsik, M. Alini, M.J. Stoddart, Epsilon-aminocaproic acid is a useful fibrin degradation inhibitor for cartilage tissue engineering, *Tissue Eng Part A* 15 (8) (2009 Aug) 2309–2313, <https://doi.org/10.1089/ten.tea.2008.0400>.
- [28] O.O. Dada, Y. Zhao, N. Jaya, O. Salas-Solano, High-resolution capillary zone electrophoresis with mass spectrometry peptide mapping of therapeutic proteins: peptide recovery and post-translational modification analysis in monoclonal antibodies and antibody–drug conjugates, *Anal. Chem.* 89 (21) (2017 Nov 7) 11236–11242, <https://doi.org/10.1021/acs.analchem.7b03643>.
- [29] X. Zhang, T. Chen, V. Li, T. Bo, M. Du, T. Huang, Cutting-edge mass spectrometry strategy based on imaged capillary isoelectric focusing (icIEF) technology for characterizing charge heterogeneity of monoclonal antibody, *Anal. Biochem.* 660 (2023 Jan) 114961, <https://doi.org/10.1016/j.ab.2022.114961>.
- [30] Z. Liu, J. Valente, S. Lin, N. Chennamsetty, D. Qiu, M. Bolgar, Cyclization of N-Terminal glutamic acid to pyro-glutamic acid impacts monoclonal antibody charge heterogeneity despite its appearance as a neutral transformation, *J Pharm Sci* 108 (10) (2019 Oct) 3194–3200, <https://doi.org/10.1016/j.xphs.2019.05.023>.
- [31] R. Gahoual, A. Burr, J.M. Busnel, L. Kuhn, P. Hammann, A. Beck, et al., Rapid and multi-level characterization of trastuzumab using sheathless capillary electrophoresis-tandem mass spectrometry, *mAbs* 5 (3) (2013 May) 479–490, <https://doi.org/10.4161/mabs.23995>.